



Published in final edited form as:

J Control Release. 2012 December 10; 164(2): 170–176. doi:10.1016/j.jconrel.2012.04.042.

Beyond the imaging: Limitations of cellular uptake study in the evaluation of nanoparticles

Emily Gullotti¹ and Yoon Yeo^{1,2,*}

¹Weldon School of Biomedical Engineering, Purdue University, 206 South Martin Jischke Drive, West Lafayette, IN 47907, USA

²Department of Industrial and Physical Pharmacy, Purdue University, 575 Stadium Mall Drive, West Lafayette, IN 47907, USA

Abstract

Poly(lactic-co-glycolic acid) (PLGA) nanoparticles (NPs) conjugated to a cell-penetrating peptide, TAT, was used to increase intracellular delivery of paclitaxel (PTX) to multi-drug resistant (MDR) cells. Efficient cellular uptake of the TAT-conjugated PLGA NPs was observed; however, it did not translate to increased killing of MDR cells. An investigation of drug release kinetics in phosphate-buffered saline containing Tween 80 led us to suspect that a significant fraction of the loaded PTX was released before efficient cellular uptake could occur. These results indicate that the increased cellular uptake of NPs does not always mean an enhanced drug effect and that it is critical to control both the location of NPs and the drug release from NPs together. Based on this study, we propose that two prevalent practices in NP research be reconsidered: First, the utility of a new NP system should be tested beyond the imaging level. Second, NP release kinetics should be monitored in a medium that can reflect the complexity of biological environment rather than a simple buffered saline.

Keywords

Polymeric nanoparticles; drug delivery; drug release; cellular uptake; bioactivity

1. Introduction

Multidrug resistance (MDR) in cancer refers to the ability of tumors to exhibit simultaneous resistance to several chemotherapeutic agents, which leads to decreased effectiveness of chemotherapy [1]. Some of the resistance is mediated by ATP-binding cassette (ABC) transporters including P-glycoprotein (Pgp) or multidrug resistance protein (MRP), which reside in cell membrane and pump out anti-cancer drugs in an ATP-dependent manner [1, 2]. Several strategies have been proposed to overcome MDR owing to the drug efflux pumps. For example, chemotherapies are combined with Pgp inhibitors [3] or genetic therapeutics such as siRNA [4] and anti-sense oligonucleotides [5, 6] to counteract the MDR effect. On the other hand, there is a good chance that their effects can be limited because of non-specificity, toxicity, or instability of such inhibitors [7–11]. In this regard, nanoparticles

© 2012 Elsevier B.V. All rights reserved.

*Corresponding author: Yoon Yeo, Ph.D., Phone: 765.496.9608, Fax: 765.494.6545, yyeo@purdue.edu.

Publisher's Disclaimer: This is a PDF file of an unedited manuscript that has been accepted for publication. As a service to our customers we are providing this early version of the manuscript. The manuscript will undergo copyediting, typesetting, and review of the resulting proof before it is published in its final citable form. Please note that during the production process errors may be discovered which could affect the content, and all legal disclaimers that apply to the journal pertain.

(NPs) have been suggested as an alternative or supplementary way of overcoming MDR [12–14].

NPs or nanocarriers are small drug carriers with a size typically ranging from 10 to 200 nm [15]. Polymeric NPs, which physically entrap drugs in solid matrix such as poly(lactic-co-glycolic acid) (PLGA), have been widely used for drug delivery to tumors due to the relatively easy preparation and size control. It has been believed that NPs entering cells can deliver anti-cancer drugs intracellularly and bypass drug efflux pumps, thereby overcoming MDR [16]. However, our previous work has shown that PLGA NPs are not readily taken up by cells, indicating that cytotoxicity of drug-carrying NPs is more likely due to a drug that has been separated from NPs extracellularly [17]. Under this scenario, PLGA NPs would be ineffective in treating MDR tumor cells. In fact, Chavanpatil et al. reported that PTX carried by PLGA NPs was also subject to a Pgp-mediated MDR [18].

Therefore, we propose to overcome MDR using PLGA NPs decorated with a cell-penetrating peptide, which facilitates cellular uptake of NPs [19] and thus intracellular drug delivery. Of several cell-penetrating peptides, the TAT peptide, a membrane-translocating peptide sequence (RKKRRQRRR) of the HIV TAT protein, has been frequently used to transport a variety of NPs across cell membranes [19–23]. The TAT peptide is reported to have low cytotoxicity and a high affinity for cell membranes irrespective of cell types [23]. Therefore, TAT peptide is expected to be an efficient ligand to enhance cellular uptake of polymeric NPs and their intracellular drug delivery to MDR cells.

To test feasibility of this approach, we synthesized a conjugate of PLGA and TAT peptide and created NPs. The NPs were examined with respect to the ability to enter ovarian cancer cells and deliver paclitaxel (PTX), a substrate of Pgp, to drug-resistant cells. Based on these results, the contribution of NP uptake to overcoming MDR was investigated.

2. Materials and Methods

2.1 Materials

PTX was a gift from Samyang Genex Corp. (Seoul, Korea). PLGA (LA:GA = 50:50, carboxylic acid end group, viscosity range: 0.15–0.25 dL/g, molecular weight: 4.2 kDa according to the vendor) was purchased from Lactel Absorbable Polymers (Durect Corporation, AL, USA). TAT peptide (GRKKRRQRRRGYKC-NH₂) was purchased from Biomatik (Cambridge, Ontario, Canada) or New England Peptide (MA, USA). N-succinimidyl 4-(4-maleimidophenyl) butyrate (SMPB) was purchased from Thermo Fisher Scientific (Rockford, IL, USA) or Sigma Aldrich (St. Louis, MO, USA). Inject maleimide conjugation buffer was also purchased from Thermo Fisher Scientific (Rockford, IL, USA). Polyvinyl alcohol (6,000 Da) was purchased from Polysciences, Inc (Warrington, PA, USA). All other materials were purchased from Sigma Aldrich (St. Louis, MO, USA), unless otherwise specified.

2.2 PLGA-TAT conjugation (Scheme 1)

PLGA-TAT was created using a method adapted from Nam et al. [19]. Relatively low molecular weight PLGA was used to afford a large number of carboxyl groups to modify with TAT peptide. First, amine-terminated PLGA (PLGA-NH₂) was prepared. Briefly, PLGA and hydroxybenotriazole (HOBt) (in a 1:2 molar ratio) was dissolved in water-free dioxane under argon. To this mixture, 1-ethyl-3-(3-dimethylaminopropyl) carbodiimide (EDC) and triethylamine (TEA) were added dropwise in molar ratios of 3:1 and 6:1, respectively, relative to PLGA. After one hour of reaction under stirring, a ten-fold molar excess of hexamethylene diamine (HMDA) (relative to PLGA) dissolved in a small amount of dioxane was added dropwise to the reaction. The cloudy reaction cleared up within a few

hours and was spun overnight. Dioxane was then evaporated, and the product (PLGA-NH₂) was redissolved in dichloromethane (DCM). PLGA-NH₂ was purified by repeated precipitation in a mixture of methanol and ethyl ether. Conjugation yield was determined by ¹H-NMR.

The purified PLGA-NH₂ was reacted with a two-fold molar excess of SMPB to create maleimide-terminated PLGA. Briefly, PLGA-NH₂ and SMPB was dissolved in water-free DCM under argon and allowed to react overnight. The product was purified by alternating dissolution in DCM and precipitation in ethyl ether multiple times. Removal of excessive SMPB was verified by thin layer chromatography (TLC). The final conjugation yield was determined with ¹H-NMR.

Finally, the maleimide-terminated PLGA was reacted with the sulfhydryl group on the cysteine of TAT peptide in a molar ratio of 1:1. The TAT peptide was dissolved in 400 μL of inject maleimide conjugation buffer and added dropwise to the maleimide-terminated PLGA dissolved in dimethyl sulfoxide (DMSO). The reaction proceeded overnight. Excess TAT peptide was removed by dialysis against water. The water was replaced four times every 6–8 hours. After dialysis, the polymer was freeze-dried and stored at –20°C.

2.3 Nanoparticle formation

To make PLGA NPs, 20 mg of PLGA was dissolved in 600 μL of DCM. For TAT-containing NPs (PLGA-TAT NPs) or fluorescently labeled NPs (PLGA* or PLGA*-TAT NPs), 5 mg of PLGA-TAT and/or fluoresceinamine-conjugated PLGA (PLGA*) were added to replace an equivalent amount of PLGA [17]. NPs loaded with PTX (PTX/PLGA NPs or PTX/PLGA-TAT NPs) were prepared by replacing 2 mg of PLGA with 2 mg of PTX (theoretical drug loading: 10%). To prepare NPs loaded with curcumin (Cur/PLGA NPs), 2 mg of curcumin (Cur) dissolved in 60 μL of DMSO was added to 18 mg of PLGA dissolved in 540 μL of DCM and mixed by vortexing.

The polymer or drug/polymer mixture solution was added to 2 mL of a 5% polyvinyl alcohol solution and immediately homogenized using a Sonics Vibracell™ probe sonicator for 1 minute, pulsing 4 seconds on and 2 seconds off at an amplitude of 80%. The sonication time was increased to 6 minutes for PLGA-TAT NPs. After sonication, the NP solution was added to 5 mL of deionized water and spun overnight to evaporate the remaining DCM. The NPs were then collected via centrifugation at 10,000 rpm for 1 hour at 4°C and washed twice in deionized water with centrifugation at 8,000 rpm for 30 minutes at 4°C. An NP pellet was collected at the end of the second wash and used in less than 24 hours after preparation.

2.4 Characterization of the NPs

Size and zeta potential of NPs were determined using a Malvern Zetasizer Nano ZS90 (Worcestershire, UK). For the measurement, NPs were diluted in phosphate buffer (1 mM, pH 7.4) to make a 0.5 mg/mL suspension.

To determine the loading efficiency (LE, weight percentage of drug in NPs) of PTX-loaded NPs, a known weight of NPs was dissolved in 1 mL of a 50:50 mixture of acetonitrile (ACN) and water and analyzed via high pressure liquid chromatography (HPLC). HPLC was performed with HPLC 1100 series (Agilent Technologies, Palo Alto, CA, USA) and Ascentis C18 column (25 cm × 4.6 mm, particle size 5 μm, Supelco, MO, USA). The mobile phase was a 50:50 mixture of ACN and water and flowed at 1 mL/min. The PTX peak was observed using a UV detector at 227 nm with a retention time of 11 min.

To determine the LE of Cur-loaded NPs, a known weight of NPs was dissolved in 1 mL of DMSO and analyzed with respect to the fluorescence of Cur in the solution (Ex: 485 nm; Em: 538 nm) using a SpectraMax M3 microplate reader (Molecular Device, Sunnyvale, CA).

2.5 Release Kinetics

PTX/PLGA NPs or PTX/PLGA-TAT NPs equivalent to 8.75 μg or 3 μg of PTX were suspended in 1 mL of phosphate-buffered saline (PBS, 10 mM phosphate, pH 7.4) with or without 0.2% Tween 80 and incubated at 37°C with rotation. At designated time points, the NP suspensions were centrifuged at 10,000 rpm for 10 minutes at 4°C. Eight hundred microliters of supernatant was sampled and replaced with fresh buffer. The NPs were resuspended with vortexing and further incubated. The supernatants were analyzed via HPLC.

2.6 Cell culture

NCI/ADR-RES ovarian cancer cells (NCI, Frederick, MD, USA), multidrug-resistant due to Pgp and MDR1 [24–27], were cultured in DMEM/F12 medium without phenol red (Invitrogen, Carlsbad, CA, USA) supplemented with 10% fetal bovine serum (FBS) and 100 units/mL penicillin and 100 $\mu\text{g}/\text{mL}$ streptomycin. SKOV-3 ovarian cancer cells (drug-sensitive cells) (ATCC) were cultured in complete RPMI-1640 medium supplemented with 10% FBS, 100 units/mL penicillin and 100 $\mu\text{g}/\text{mL}$ streptomycin. At 70–80% confluency the cells were subcultured at a ratio of 1:20. NCI/ADR-RES cells between P5 and P10 were used to maintain MDR.

2.7 Confocal imaging of NP uptake

SKOV-3 or NCI/ADR-RES cells were plated in 35 mm dishes at a density of 80,000 cells/ cm^2 or 100,000 cells/ cm^2 , respectively. After 24 hours, the medium was replaced with 2 mL of fresh complete medium containing 0.1 mg/mL PLGA*, PLGA*-TAT, or Cur/PLGANPs. Free Cur was added to the cell culture medium as a Cur/DMSO solution providing a comparable level of Cur to Cur/PLGA NPs (final DMSO concentration was less than 1%).

After 3 hours of incubation, the NP-containing medium was replaced with 2 mL of serum-free medium. For nuclear staining, 1 μL of Draq5 (Biostatus Limited, UK) was added prior to imaging. Cells were imaged with Olympus X81 confocal microscope equipped with argon FV5-LA-MAR lasers. PLGA* and PLGA*-TAT NPs were excited with a 488-nm laser, and their emission was read from 500 to 600 nm and expressed in green. Free Cur or Cur/PLGA NPs were also excited with a 488-nm laser and their emission was read from 492 to 560 nm and expressed in green. Cell nuclei were excited with a 633-nm laser, and its emission was read from 650 to 750 nm and expressed in blue. Images were processed with Olympus FLUOVIEW Ver 1.5 software (Olympus, Japan).

2.8 Cytotoxicity test

Cytotoxicity of PTX encapsulated in NPs was tested using the MTT (3-(4,5-Dimethylthiazol-2-yl)-2,5-diphenyltetrazolium bromide) assay. Cells were plated in a 96-well plate at a density of 8,000 cells per well in 200 μL of complete medium. After 24 hours, 2 μL of the concentrated NP suspension was added to each well to provide PTX in the final concentration ranging from 1 to 10,000 nM. Free PTX or blank NPs (NPs with no drug) of comparable concentrations were tested in parallel. In the case of free PTX, 2 μL of PTX solution in DMSO was added to each well. The control cells were treated with 2 μL of DMSO, which did not influence the cell viability. After incubation for 3 days, the medium was replaced with 100 μL of fresh medium and 15 μL of 5 mg/mL MTT solution and

incubated for 3.5 hours. One hundred microliters of solubilization/stop solution was then added, and the plate was left in dark overnight. The absorbance of solubilized formazan in each well was read with a microplate reader at a wavelength of 562 nm. The measured absorbance was normalized to the absorbance of control cells, which did not receive PTX.

2.9 Statistical Analysis

All data were expressed as mean \pm standard deviation. Statistics were performed using ANOVA with a Tukey test for means comparison. A value of $p < 0.05$ was considered statistically significant.

3. Results

3.1 PLGA-TAT conjugation

Synthesis of PLGA-NH₂ was confirmed by the appearance of ¹H-NMR peaks at 1.3 and 2.5 ppm. Fifty to a hundred percent of PLGA was conjugated with HMDA. Synthesis of maleimide-terminated PLGA was confirmed by the ¹H-NMR peak at 6.85 ppm. The SMPB conjugation yield was 25–60%. The production yield of PLGA-TAT was ~10%.

3.2 Characterization of PLGA NPs

The average diameter of blank PLGA NPs was 170 nm (Table 1). PLGA-TAT NPs tended to aggregate after repeated washing, probably due to the relative hydrophilicity of the polymer, which led to higher water content and plasticity of the NP matrix [28]. Therefore, additional sonication time was applied to reduce the initial NP size so that the final size after purification was comparable to that of PLGA NPs. The addition of PTX resulted in slight increase in the average size of NPs, likely due to the increased hydrophobic interactions followed by NP aggregation. NP surface charges were consistently negative, irrespective of the presence of the TAT peptide.

LEs of PTX/PLGA NPs and PTX/PLGA-TAT NPs were $16.7 \pm 4.3\%$ ($n=7$) and $4.6 \pm 1.6\%$ ($n=5$), respectively. The LE of PTX/PLGA NPs was higher than the theoretical LE (10%), which may be attributable to selective loss of PLGA during NP formation and purification. The relatively low LE of PTX/PLGA-TAT NPs suggests that the PTX loss outweighed the polymer loss, due to the presence of TAT peptide, which was hydrophilic and thus incompatible with PTX.

3.3 Cellular uptake of NPs

PLGA* NPs and PLGA*-TAT NPs were used in imaging their cellular uptake. To avoid an imaging artifact due to a dye separated from the polymer [17], a fluorescent dye (fluoresceinamine) was incorporated by covalent conjugation to PLGA instead of physical entrapment. Sizes and zeta potentials were 189 ± 17 nm and -7.1 ± 2 mV for PLGA* NPs ($n=3$), and 292 ± 59 nm and -12 ± 11 mV for PLGA*-TAT NPs ($n=4$).

SKOV-3 cells incubated with PLGA* NPs showed relatively low green fluorescence (Fig. 1A), indicating a lack of NP uptake, consistent with previous reports [17, 19]. In contrast, PLGA*-TAT NPs showed much stronger fluorescence, which indicated the presence of NPs remaining with the cells. Individual NP could not be resolved by confocal microscopy. However, the fact that fluorescence signal was found surrounding the nucleus (Supporting Fig. 1) and that the NP signals were seen on a z-section with the largest nucleus images suggested that most NPs were located within the cells. NCI/ADR-RES cells showed a similar trend (Fig. 1B). The cells incubated with PLGA* NPs showed no green fluorescence, whereas those with PLGA*-TAT NPs exhibited a strong fluorescence signal of internalized NPs.

3.4 Cytotoxicity of PTX/PLGA-TAT NPs on SKOV-3 and NCI/ADR-RES Cells

NPs containing PTX were incubated for 3 days with SKOV-3 and NCI/ADR-RES cells to determine the contribution of their cellular uptake to the cell killing effect. Blank NPs (PLGA and PLGA-TAT NPs) were also tested in parallel and found to have a modest level of toxicity at higher concentrations in both cells, which would be attributable to the inherent toxicity of the low molecular weight PLGA [29].

SKOV-3 cells were sensitive to PTX and exhibited similar dose-responses to free PTX, PTX/PLGA NPs, and PTX/PLGA-TAT NPs (Fig. 2A). There was no significant difference between the two NPs attributable to the presence of TAT. In the case of drug-resistant NCI/ADR-RES cells, PTX had an insignificant effect on cell toxicity at concentrations below 1000 nM, as expected (Fig. 2B). PTX/NPs (PTX/PLGA NPs and PTX/PLGA-TAT NPs) were relatively toxic but not more than blank NPs. Therefore, most toxicity of PTX/NPs appeared due to the NPs rather than PTX carried by the NPs. PTX/PLGA-TAT NPs were not significantly more toxic than PTX/PLGA NPs at any concentrations.

3.5 Release Kinetics of PTX/PLGA NPs

PTX release from PTX/PLGA NPs was first tested in PBS with no surfactant. According to the PTX solubility (1–3 $\mu\text{g/mL}$) determined in previous studies [17, 30] and typical release profiles of PTX-loaded PLGA NPs [31–33], the NP concentrations (equivalent to 3 $\mu\text{g/mL}$ PTX) were expected to be low enough to allow unlimited release of PTX. However, no significant PTX release was observed in PBS after an initial 20% release in the first 4 hours. It was separately observed that 3 $\mu\text{g/mL}$ PTX precipitated in 30 min upon incubation in PBS and was not recovered in supernatant (data not shown). To prevent precipitation of the released PTX without increasing the volume of release medium, the release studies were performed using PBS containing 0.2% Tween 80. Here, PTX/PLGA and PTX/PLGA-TAT NPs released ~60% of the encapsulated drug in less than 3 hours (Fig. 3).

3.6 Cellular uptake of curcumin (Cur) encapsulated in NPs

To observe cellular uptake of drug carried by NPs, PLGA NPs encapsulating Cur (Cur/PLGA NPs) were incubated with SKOV-3 or NCI/ADR-RES cells and imaged on confocal microscopy. Cur was used instead of PTX because it can be directly visualized by fluorescence (Ex: 488 nm; Em: 492–560 nm). Cur is also poorly soluble in water (solubility: ~20 $\mu\text{g/mL}$ [34]). Cur/PLGA NPs had an average size and zeta potential of 154 ± 4.4 nm and -12 ± 2.2 mV, respectively. The average LE was $4.3 \pm 1.5\%$. For comparison, free Cur was added at approximately the same drug concentration as the NPs (assuming a LE of 3.6%). In 3 hours SKOV-3 cells incubated with free Cur showed a large amount of intracellular Cur signal indicating cellular uptake of Cur (Fig. 4A left). SKOV-3 cells incubated with Cur/PLGA NPs also showed a strong intracellular Cur signal (Fig. 4A right). A similar result was obtained with NCI-ADR/RES cells. Although dimmer than the signals in SKOV-3 cells, intracellular fluorescence was clearly observed in NCI/ADR-RES cells incubated with either free Cur (Fig. 4B left) or Cur/PLGA NPs (Fig. 4B right).

4. Discussion

NP-mediated intracellular drug delivery has been considered a promising way of bypassing MDR. Several ligands that promote cell-NP interactions, such as cell-penetrating peptides, folate, transferrin, aptamers, and antibodies have been employed to aid in the intracellular delivery of NPs [35, 36]. Here a general expectation is that the cell-interactive ligands will increase cellular uptake of NPs and have them release the encapsulated chemotherapeutic drugs intracellularly, where the drug can kill the cell before the MDR machinery can remove it [13, 37]. In many studies dealing with cell-interactive NPs, images and quantities of NPs

taken up by target cells are the most important and encouraging results, heralding the anticipated intracellular effects, which are however often left untested [38–48]. In this study, we intended to investigate how the enhanced NP-cell interactions translate to drug activity in cancer cells, especially those exhibiting MDR, using PLGA NPs as a model carrier.

We chose TAT peptide as a cell-interactive ligand, which has proven effective in facilitating cellular uptake of micelles or liposomes [37, 49, 50], in modifying PLGA NPs. Surface charge of PLGA-TAT NPs was dominated by carboxyl groups of PLGA rather than positively charged TAT peptide, which indicates low density of TAT peptide on the NP surface. Nonetheless, PLGA-TAT NPs were taken up by SKOV-3 and NCI/ADR-RES cells in 3 hours unlike bare PLGA NPs, demonstrating the potency of TAT peptide as a cell-interactive ligand. Based on these results, we anticipated that PTX carried by PLGA-TAT NPs would be effective in killing MDR cells.

For PTX-sensitive SKOV-3 cells, we observed no increase in overall cytotoxicity by PTX/PLGA-TAT NPs as compared to free PTX or PTX/PLGA NPs. This result could be readily explained since the location of a drug source (extracellular vs. intracellular) should not make much difference in drug-sensitive cells. Here, PTX present outside the cells (free PTX, PTX/PLGA NPs) would enter the cells without limitation and act on the intracellular target just like the drug released in the cells (PTX/PLGA-TAT NPs). On the other hand, PTX/PLGA-TAT NPs was expected to have an advantage over PTX/PLGA NPs in NCI/ADR-RES cells. In MDR cells, PTX released extracellularly from PTX/PLGA NPs, which do not enter cells, would be recognized by drug efflux pumps and removed from the cells like free PTX. In contrast, PTX released from PLGA-TAT NPs within the cells was expected to effectively avoid such removal. However, we did not observe such difference in cytotoxicity between PTX/PLGA NPs and PTX/PLGA-TAT NPs in NCI/ADR-RES cells.

To explain the lack of cytotoxic advantage of PTX/PLGA-TAT NPs over free PTX or PTX/PLGA NPs, we examined the kinetics of PTX release from the NPs. The results varied with the release medium. In PBS, a popular release medium used in many studies of PTX-loaded NPs [31–33, 51], 20% of the loaded PTX was released in 4 hours and no significant release followed. Given that 3 µg/mL PTX solution in PBS rapidly precipitated at 37°C (data not shown), the limited PTX release was attributable to its low solubility in PBS. On the other hand, in PBS containing 0.2% Tween 80, which helped solubilize the released PTX, 60% of the encapsulated drug was released from the NPs in less than 3 hours, a time frame we found necessary to achieve significant cellular uptake (Supporting Fig. 2). It is not clear how well PBS with 0.2% Tween 80 resembles extracellular environment. However, given that complete medium contains various hydrophobic and amphiphilic components such as proteins and lipids, one can imagine that the PTX release in cell culture may be better simulated by PBS with 0.2% Tween 80 than by simple PBS. Under this assumption, the rapid PTX release observed in PBS with 0.2% Tween 80 indicates that most of the encapsulated PTX had been released extracellularly before the majority of PLGA-TAT NPs were taken up by the cells. This extracellular drug release is consistent with the lack of cytotoxicity difference among free PTX and PTX/NPs in the sensitive SKOV-3 cells. Importantly, this rapid extracellular release explains the lack of cytotoxic advantage of PTX/PLGA-TAT NPs in NCI/ADR-RES cells.

To further confirm the extracellular drug release from NPs, we incubated cells with PLGA NPs or PLGA-TAT NPs loaded with a fluorescent drug (Cur) and observed drug distribution in the cells. Both SKOV-3 and NCI/ADR-RES cells showed intracellular fluorescence in 3 hours of incubation with NPs, similar to those with free Cur (Fig. 4). Given that NP uptake by these cells during the same period was little to none (Fig. 1 left), the intracellular Cur signal shown in the cells can be only explained by the extracellular release of Cur.

These results show that the uptakes of a drug and a carrier do not necessarily coincide unless the drug release is simultaneously modulated. Therefore, the increased cellular uptake of a drug carrier does not always translate to an enhanced drug effect. Accordingly, we find it necessary to reconsider at least two prevalent practices in NP-based drug delivery research. First, the utility of a new NP system should be tested beyond the imaging level. While cellular uptake is an important step that can potentially improve drug delivery to MDR cells, it should be accompanied by a timely control of drug release in order to achieve desired activity. Second, one must consider the limitation of PBS as a release medium in predicting the kinetics of drug release in biological environment. In our study PTX encapsulated in the NPs was indistinguishable from free PTX most likely due to the rapid drug release in the complete culture medium. This release behavior was not predicted in simple PBS, where the released PTX was quickly precipitated leaving little PTX in a dissolved form. In the current research practice, the lack of detectable drug in PBS is often interpreted as stability of the NP system.

This study demonstrates instability of PLGA NP systems in biological environment. Similar limitations have been previously noted with other types of NPs *in vivo*. In a recent study of doxorubicin-encapsulated liposomes, the carrier (liposomes) showed a very different pharmacokinetics than doxorubicin, suggesting premature leakage of doxorubicin from the liposomes during circulation [52]. Similarly, polymeric micelles made of polyethylene glycolpolylactic acid block copolymer were found to dissociate within 15 minutes of intravenous injection and release the entrapped dyes [53]. When this happens, the remaining treatment becomes equivalent to a simple mixture of free drug and empty carriers or the components, and any advantage of drug encapsulation will be quickly lost, as demonstrated in our study *in vitro*. Therefore, an ability to retain a drug until it reaches a target location is one of the most significant (yet often neglected) attributes of an NP. Future work on NP systems must focus on stabilizing the drug carrier in biological environment. To this end, a new test condition that can reliably predict the stability of NPs is urgently needed.

5. Conclusions

NPs have the potential to improve chemotherapy by controlling spatiotemporal availability of an anticancer drug. PLGA-TAT NPs, which could readily enter cells, were expected to overcome MDR by bypassing drug efflux pumps, but the expected cytotoxic advantage was not observed due to the premature drug release. This result highlights the importance of controlling the location of NPs and timing of drug release simultaneously. Therefore, we suggest that a new NP system should be evaluated not only on an imaging level but also for the ability to control the drug release in a biologically relevant condition, to ensure that the carrier will deliver a drug in a right place and a right time for the desired therapeutic response.

Supplementary Material

Refer to Web version on PubMed Central for supplementary material.

Acknowledgments

The authors would like to thank Zohreh Amoozgar for invaluable assistance with the polymer modification and Mark Hamilton for help with the MTT assays. Financial support was provided by NIH R21 CA135130 (YY), the P.E.O. Scholar Award (EG), and the Bilsland Dissertation Fellowship (EG).

References

1. Krishna R, Mayer LD. Multidrug resistance (MDR) in cancer - Mechanisms, reversal using modulators of MDR and the role of MDR modulators in influencing the pharmacokinetics of anticancer drugs. *Eur. J. Pharm. Sci.* 2000; 11(4):265–283. [PubMed: 11033070]
2. Borst P, Evers R, Kool M, Wijnholds J. A family of drug transporters: the multidrug resistance-associated proteins. *J. Natl. Cancer I.* 2000; 92(16):1295–1302.
3. Liu Y, Huang L, Liu F. Paclitaxel Nanocrystals for Overcoming Multidrug Resistance in Cancer. *Mol. Pharmaceut.* 2010; 7(3):863–869.
4. Yadav S, van Vlerken LE, Little SR, Amiji MM. Evaluations of combination MDR-1 gene silencing and paclitaxel administration in biodegradable polymeric nanoparticle formulations to overcome multidrug resistance in cancer cells. *Cancer Chemoth. Pharm.* 2009; 63(4):711–722.
5. Wang Y, Saad M, Pakunlu RI, Khandare JJ, Garbuzenko OB, Vetcher AA, Soldatenkov VA, Pozharov VP, Minko T. Nonviral nanoscale-based delivery of antisense oligonucleotides targeted to hypoxia-inducible factor 1 alpha enhances the efficacy of chemotherapy in drug-resistant tumor. *Clin. Cancer Res.* 2008; 14(11):3607–3616. [PubMed: 18519795]
6. Pakunlu RI, Wang Y, Saad M, Khandare JJ, Starovoytov V, Minko T. In vitro and in vivo intracellular liposomal delivery of antisense oligonucleotides and anticancer drug. *J. Control. Release.* 2006; 114(2):153–162. [PubMed: 16889867]
7. Thomas H, Coley HM. Overcoming multidrug resistance in cancer: an update on the clinical strategy of inhibiting p-glycoprotein. *Cancer Control.* 2003; 10(2):159–165. [PubMed: 12712010]
8. Kannan P, Telu S, Shukla S, Ambudkar SV, Pike VW, Halldin C, Gottesman MM, Innis RB, Hall MD. The "Specific" P-Glycoprotein Inhibitor Tariquidar Is Also a Substrate and an Inhibitor for Breast Cancer Resistance Protein (BCRP/ABCG2). *ACS Chem. Neurosci.* 2011; 2(2):82–89. [PubMed: 22778859]
9. Curcio LD, Bouffard DY, Scanlon KJ. Oligonucleotides as modulators of cancer gene expression. *Pharmacol. Therapeut.* 1997; 74(3):317–332.
10. Devi GR. siRNA-based approaches in cancer therapy. *Cancer Gene Ther.* 2006; 13(9):819–829. [PubMed: 16424918]
11. Tong AW, Zhang YA, Nemunaitis J. Small interfering RNA for experimental cancer therapy. *Curr. Opin. Mol. Ther.* 2005; 7(2):114–124. [PubMed: 15844618]
12. Brigger I, Dubernet C, Couvreur P. Nanoparticles in cancer therapy and diagnosis. *Adv. Drug Deliv. Rev.* 2002; 54(5):631–651. [PubMed: 12204596]
13. Goren D, Horowitz AT, Tzemach D, Tarshish M, Zalipsky S, Gabizon A. Nuclear delivery of doxorubicin via folate-targeted liposomes with bypass of multidrug-resistance efflux pump. *Clin. Cancer Res.* 2000; 6(5):1949–1957. [PubMed: 10815920]
14. Kim D, Lee ES, Oh KT, Gao ZG, Bae YH. Doxorubicin-loaded polymeric micelle overcomes multidrug resistance of cancer by double-targeting folate receptor and early endosomal pH. *Small.* 2008; 4(11):2043–2050. [PubMed: 18949788]
15. Yokoyama M. Drug targeting with nano-sized carrier systems. *J. Artif. Organs.* 2005; 8(2):77–84. [PubMed: 16094510]
16. Sahoo SK, Labhasetwar V. Enhanced antiproliferative activity of transferrin-conjugated paclitaxel-loaded nanoparticles is mediated via sustained intracellular drug retention. *Mol. Pharmaceut.* 2005; 2(5):373–383.
17. Xu P, Gullotti E, Tong L, Highley CB, Errabelli DR, Hasan T, Cheng J-X, Kohane DS, Yeo Y. Intracellular drug delivery by poly(lactic-co-glycolic acid) nanoparticles, revisited. *Mol. Pharmaceut.* 2009; 6(1):190–201.
18. Chavanpatil MD, Patil Y, Panyam J. Susceptibility of nanoparticle-encapsulated paclitaxel to P-glycoprotein-mediated drug efflux. *Int. J. Pharmaceut.* 2006; 320(1–2):150–156.
19. Nam YS, Park JY, Han SH, Chang IS. Intracellular drug delivery using poly(D,L-lactide-co-glycolide) nanoparticles derivatized with a peptide from a transcriptional activator protein of HIV-1. *Biotechnol. Lett.* 2002; 24(24):2093–2098.
20. Torchilin VP. Tat peptide-mediated intracellular delivery of pharmaceutical nanocarriers. *Adv. Drug Deliv. Rev.* 2008; 60(4–5):548–558. [PubMed: 18053612]

21. Torchilin VP, Rammohan R, Weissig V, Levchenko TS. TAT peptide on the surface of liposomes affords their efficient intracellular delivery even at low temperature and in the presence of metabolic inhibitors. *Proc. Natl. Acad. Sci. USA*. 2001; 98(15):8786–8791. [PubMed: 11438707]
22. Koch AM, Reynolds F, Merkle HP, Weissleder R, Josephson L. Transport of surface-modified nanoparticles through cell monolayers. *ChemBioChem*. 2005; 6(2):337–345. [PubMed: 15651046]
23. Berry CC. Intracellular delivery of nanopartides via the HIV-1 tat peptide. *Nanomedicine-UK*. 2008; 3(3):357–365.
24. Alvarez M, Paull K, Monks A, Hose C, Lee JS, Weinstein J, Grever M, Bates S, Fojo T. Generation of a drug resistance profile by quantitation of mdr-1/P-glycoprotein in the cell lines of the National Cancer Institute Anticancer Drug Screen. *J. Clin. Invest.* 1995; 95(5):2205–2214. [PubMed: 7738186]
25. Lee JS, Paull K, Alvarez M, Hose C, Monks A, Grever M, Fojo AT, Bates SE. Rhodamine efflux patterns predict P-glycoprotein substrates in the National Cancer Institute drug screen. *Mol. Pharmacol.* 1994; 46(4):627–638. [PubMed: 7969041]
26. Scudiero DA, Monks A, Sausville EA. Cell line designation change: multidrug-resistant cell line in the NCI anticancer screen. *J. Natl. Cancer Inst.* 1998; 90(11):862. [PubMed: 9625176]
27. Wu L, Smythe AM, Stinson SF, Mullendore LA, Monks A, Scudiero DA, Paull KD, Koutsoukos AD, Rubinstein LV, Boyd MR, Shoemaker RH. Multidrug-resistant phenotype of disease-oriented panels of human tumor cell lines used for anticancer drug screening. *Cancer Res.* 1992; 52(11):3029–3034. [PubMed: 1350507]
28. Wischke C, Schwendeman SP. Principles of encapsulating hydrophobic drugs in PLA/PLGA microparticles. *Int. J. Pharmaceut.* 2008; 364(2):298–327.
29. Gryparis EC, Hatzia Apostolou M, Papadimitriou E, Avgoustakis K. Anticancer activity of cisplatin-loaded PLGA-mPEG nanoparticles on LNCaP prostate cancer cells. *Eur. J. Pharm. Biopharm.* 2007; 67(1):1–8. [PubMed: 17303395]
30. Yang T, Cui FD, Choi MK, Cho JW, Chung SJ, Shim CK, Kim DD. Enhanced solubility and stability of PEGylated liposomal paclitaxel: In vitro and in vivo evaluation. *Int. J. Pharm.* 2007; 338(1–2):317–326. [PubMed: 17368984]
31. Fonseca C, Simões S, Gaspar R. Paclitaxel-loaded PLGA nanoparticles: preparation, physicochemical characterization and in vitro anti-tumoral activity. *J. Control. Release.* 2002; 83(2):273–286. [PubMed: 12363453]
32. Mu L, Feng SS. A novel controlled release formulation for the anticancer drug paclitaxel (Taxol®): PLGA nanoparticles containing vitamin E TPGS. *J. Control. Release.* 2003; 86(1):33–48. [PubMed: 12490371]
33. Kang BK, Chon SK, Kim SH, Jeong SY, Kim MS, Cho SH, Lee HB, Khang G. Controlled release of paclitaxel from microemulsion containing PLGA and evaluation of anti-tumor activity in vitro and in vivo. *Int. J. Pharmaceut.* 2004; 286(1–2):147–156.
34. Yallapu MM, Jaggi M, Chauhan SC. β -Cyclodextrin-curcumin self-assembly enhances curcumin delivery in prostate cancer cells, *Colloids and Surfaces B. Biointerfaces.* 2010; 79:113–125. [PubMed: 20456930]
35. Torchilin VP. Targeted pharmaceutical nanocarriers for cancer therapy and Imaging. *AAPS J.* 2007; 9(2):E128–E147. [PubMed: 17614355]
36. Farokhzad OC, Jon S, Khademhosseini A, Tran T-NT, LaVan DA, Langer R. Nanoparticle-aptamer bioconjugates: a new approach for targeting prostate cancer cells. *Cancer Res.* 2004; 64(21):7668–7672. [PubMed: 15520166]
37. Lee ES, Gao ZG, Kim D, Park K, Kwon IC, Bae YH. Super pH-sensitive multifunctional polymeric micelle for tumor pH(e) specific TAT exposure and multidrug resistance. *J. Control. Release.* 2008; 129(3):228–236. [PubMed: 18539355]
38. Wong HL, Bendayan R, Rauth AM, Xue HY, Babakhanian K, Wu XY. A mechanistic study of enhanced doxorubicin uptake and retention in multidrug resistant breast cancer cells using a polymer-lipid hybrid nanoparticle system. *J. Pharmacol. Exp. Ther.* 2006; 317(3):1372–1381. [PubMed: 16547167]

39. Zhang L, Chan JM, Gu FX, Rhee J-W, Wang AZ, Radovic-Moreno AF, Alexis F, Langer R, Farokhzad OC. Self-assembled lipid-polymer hybrid nanoparticles: a robust drug delivery platform. *ACS Nano*. 2008; 2(8):1696–1702. [PubMed: 19206374]
40. Poon Z, Chang D, Zhao X, Hammond PT. Layer-by-layer nanoparticles with a pH-sheddable layer for in vivo targeting of tumor hypoxia. *ACS Nano*. 2011; 5(6):4284–4292. [PubMed: 21513353]
41. Hou ZQ, Zhan CM, Jiang QW, Hu Q, Li L, Chang D, Yang XR, Wang YX, Li Y, Ye SF, Xie LY, Yi YF, Zhang QQ. Both FA- and mPEG-conjugated chitosan nanoparticles for targeted cellular uptake and enhanced tumor tissue distribution. *Nanoscale Res. Lett.* 2011; 6:563. [PubMed: 22027239]
42. Langcharoen P, Punfa W, Yodkeeree S, Kasinrerak W, Ampasavate C, Anuchapreeda S, Limtrakul P. Anti-P-glycoprotein conjugated nanoparticles for targeting drug delivery in cancer treatment. *Arch. Pharm. Res.* 2011; 34(10):1679–1689. [PubMed: 22076768]
43. Song CK, Balakrishnan P, Shim CK, Chung SJ, Kim DD. Enhanced in vitro cellular uptake of P-gp substrate by poloxamer-modified liposomes (PMLs) in MDR cancer cells. *J. Microencapsul.* 2011; 28(6):575–581. [PubMed: 21770706]
44. Cao WQ, Zhou J, Wang Y, Zhu L. Synthesis and in vitro cancer cell targeting of folate-functionalized biodegradable amphiphilic dendrimer-like star polymers. *Biomacromolecules*. 2010; 11(2):3680–3687. [PubMed: 21086989]
45. Nam HY, Kwon SM, Chung H, Lee SY, Kwon SH, Jeon H, Kim Y, Park JH, Kim J, Her S, Oh YK, Kwon IC, Kim K, Jeong SY. Cellular uptake mechanism and intracellular fate of hydrophobically modified glycol chitosan nanoparticles. *J. Control. Release*. 2009; 135(3):259–267. [PubMed: 19331853]
46. Shen YQ, Zhan YH, Tang JB, Xu PS, Johnson PA, Radosz M, Van Kirk EA, Murdoch WJ. Multifunctioning pH-responsive nanoparticles from hierarchical self-assembly of polymer brush for cancer drug delivery. *AIChE J.* 2008; 54(11):2979–2989.
47. Esmaili F, Ghahremani MH, Ostad SN, Atyabi F, Seyedabadi M, Malekshahi MR, Amini M, Dinarvand R. Folate-receptor-targeted delivery of docetaxel nanoparticles prepared by PLGA-PEG-folate conjugate. *J. Drug Target*. 2008; 16(5):415–423. [PubMed: 18569286]
48. Mohajer G, Lee ES, Bae YH. Enhanced intercellular retention activity of novel pH-sensitive polymeric micelles in wild and multidrug resistant MCF-7 cells. *Pharm. Res.* 2007; 24(9):1618–1627. [PubMed: 17385015]
49. Sawant RR, Torchilin VP. Enhanced cytotoxicity of TATp-bearing paclitaxel-loaded micelles in vitro and in vivo. *Int. J. Pharmaceut.* 2009; 374(1–2):114–118.
50. Sawant RM, Hurley JP, Salmaso S, Kale A, Tolcheva E, Levchenko TS, Torchilin VP. "SMART" drug delivery systems: Double-targeted pH-responsive pharmaceutical nanocarriers. *Bioconjugate Chem.* 2006; 17(4):943–949.
51. Danhier F, Lecouturier N, Vroman B, Jérôme C, Marchand-Brynaert J, Feron O, Préat V. Paclitaxel-loaded PEGylated PLGA-based nanoparticles: In vitro and in vivo evaluation. *J. Control. Release*. 2009; 133(1):11–17. [PubMed: 18950666]
52. de Smet M, Heijman E, Langereis S, Hijnen NM, Grull H. Magnetic resonance imaging of high intensity focused ultrasound mediated drug delivery from temperature-sensitive liposomes: An in vivo proof-of-concept study. *J. Control. Release*. 2011; 150(1):102–110. [PubMed: 21059375]
53. Chen H, Kim S, He W, Wang H, Low PS, Park K, Cheng JX. Fast release of lipophilic agents from circulating PEG-PDLLA micelles revealed by in vivo Forster resonance energy transfer imaging. *Langmuir*. 2008; 24(10):5213–5217. [PubMed: 18257595]

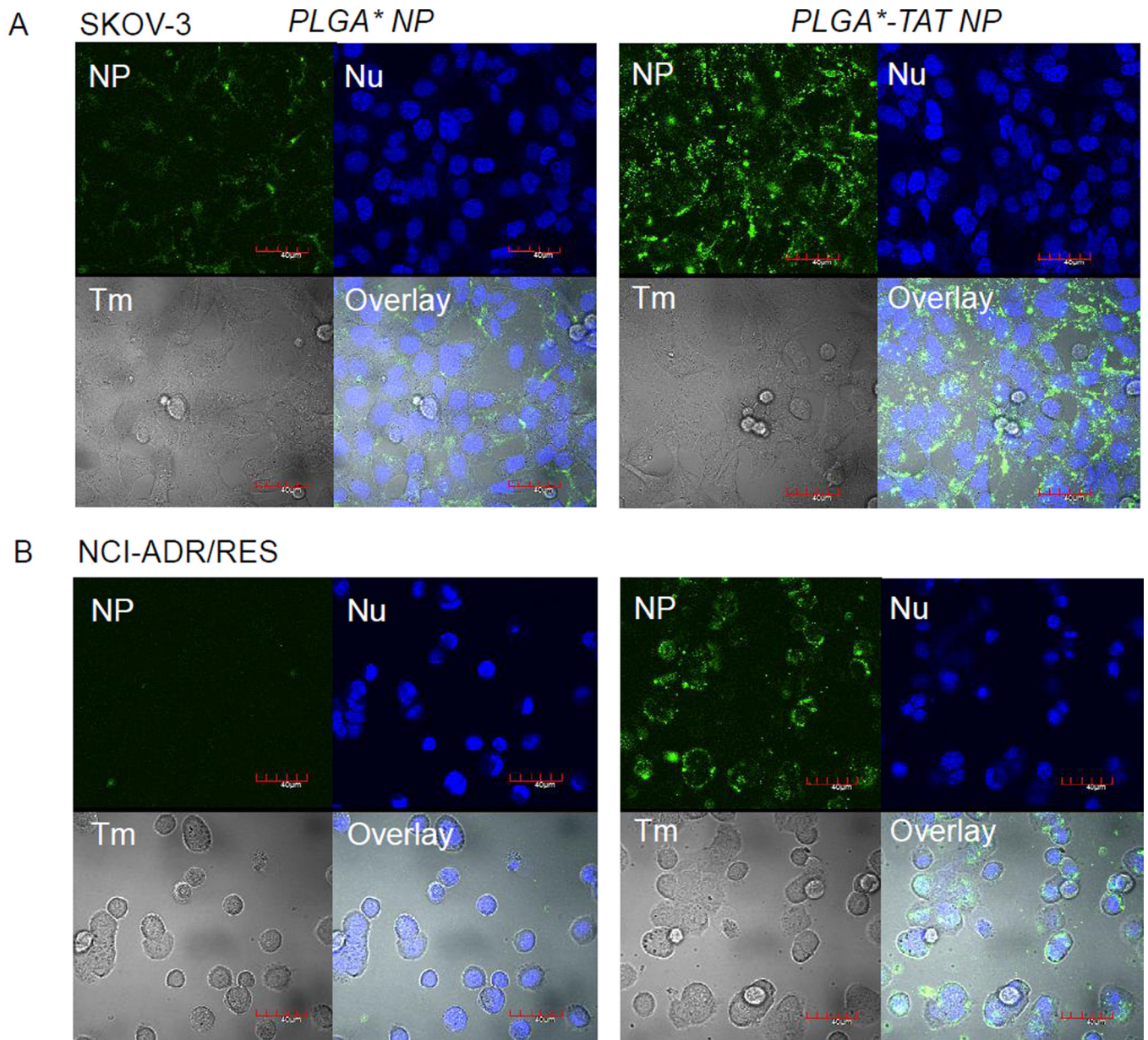


Fig. 1. (A) SKOV-3 cells and (B) NCI/ADR-RES cells incubated with fluorescently labeled NPs for 3 hours. PLGA*-TAT NPs entered the cells more effectively than those lacking TAT peptide, PLGA* NPs. NP: green fluorescence signal from NPs; Nu: nuclei stained with Draq5; Tm: transmission image; Overlay: overlay of NP, Nu and Tm. Magnification: 600 \times . Scale bar: 40 μ m.

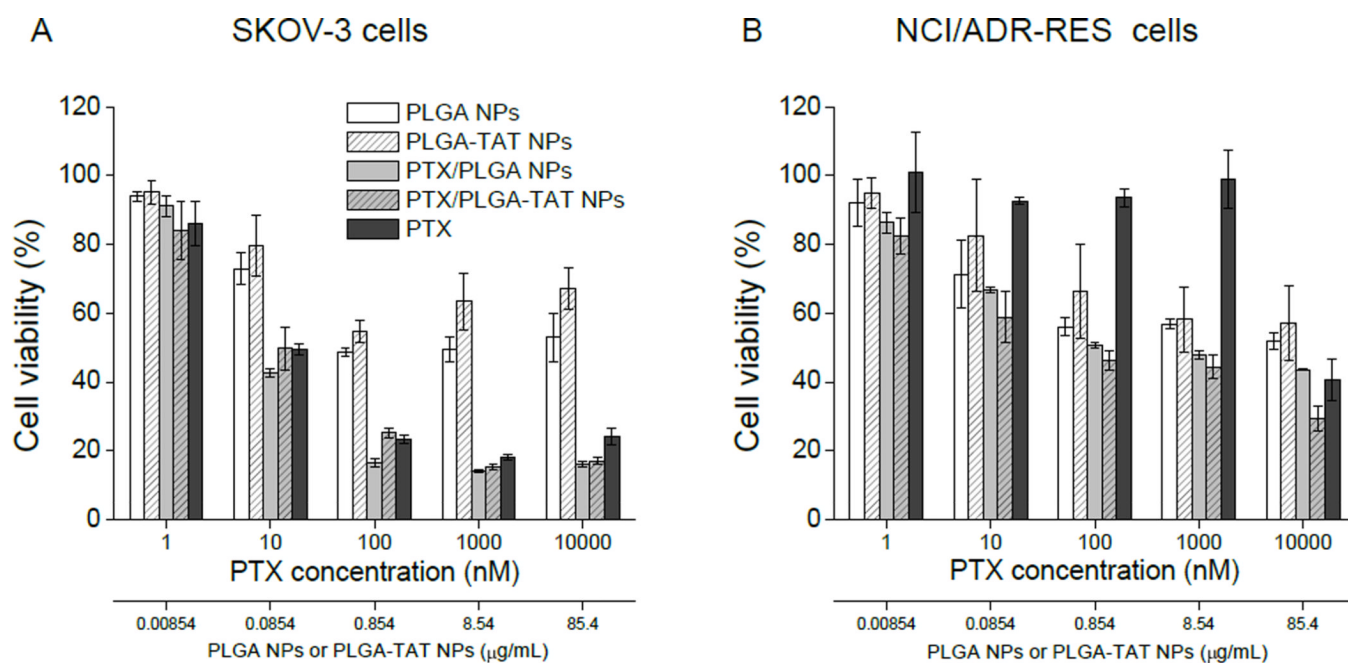


Fig. 2. MTT assays on (A) SKOV-3 cells and (B) NCI/ADR-RES cells. PTX/NPs (PTX/PLGA NPs and PTX/PLGA-TAT NPs) with average LEs from 5–20% were added to provide PTX concentrations ranging from 1 to 10,000 nM. Blank NPs (PLGA NPs and PLGA-TAT NPs) were added to provide the same amounts of NPs as PTX/NPs with 10% LE.

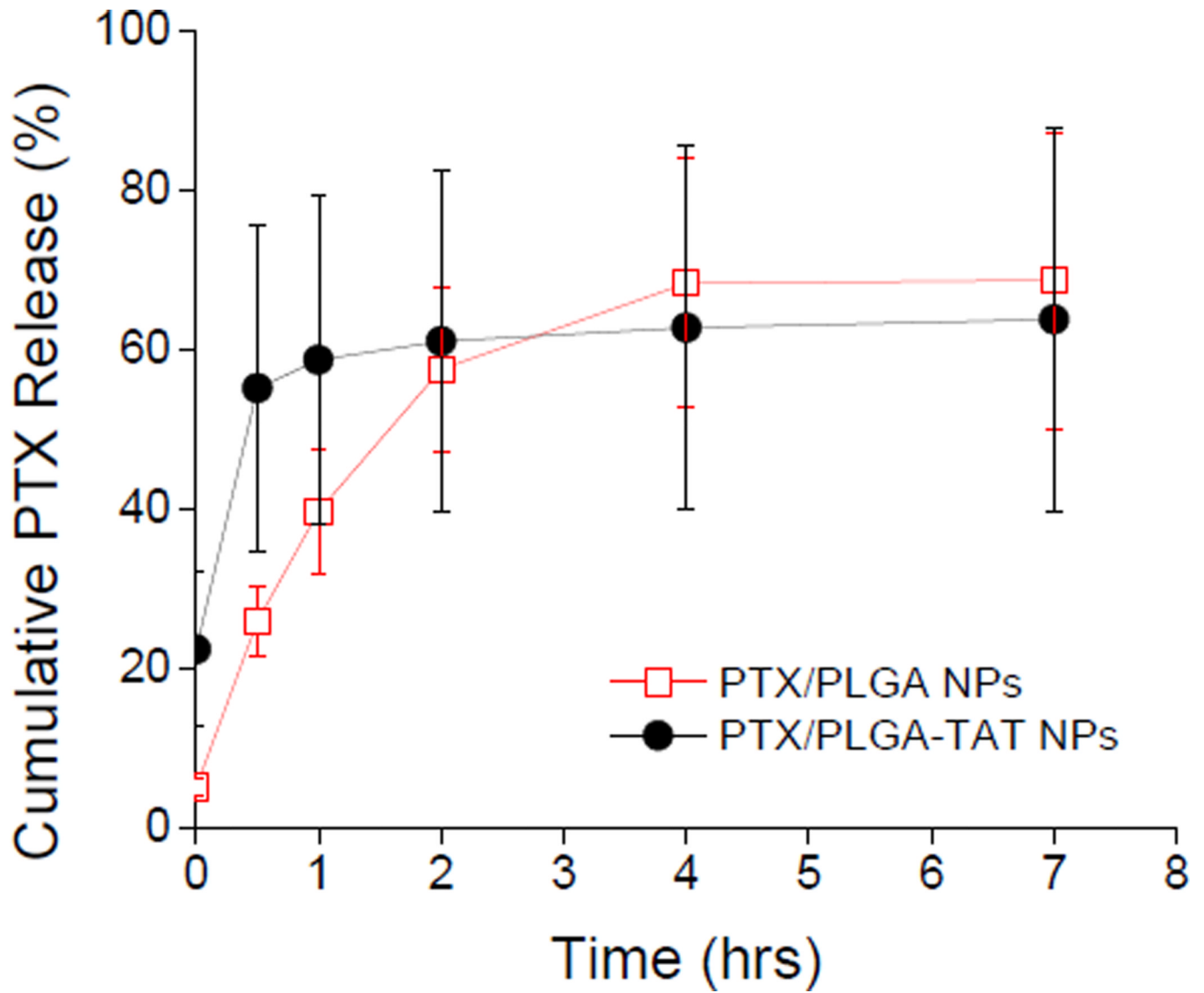


Fig. 3. Release kinetics of PTX/NPs in PBS containing 0.2% Tween 80. Each data point represents an average and standard deviation of at least 3 identically and independently prepared samples.

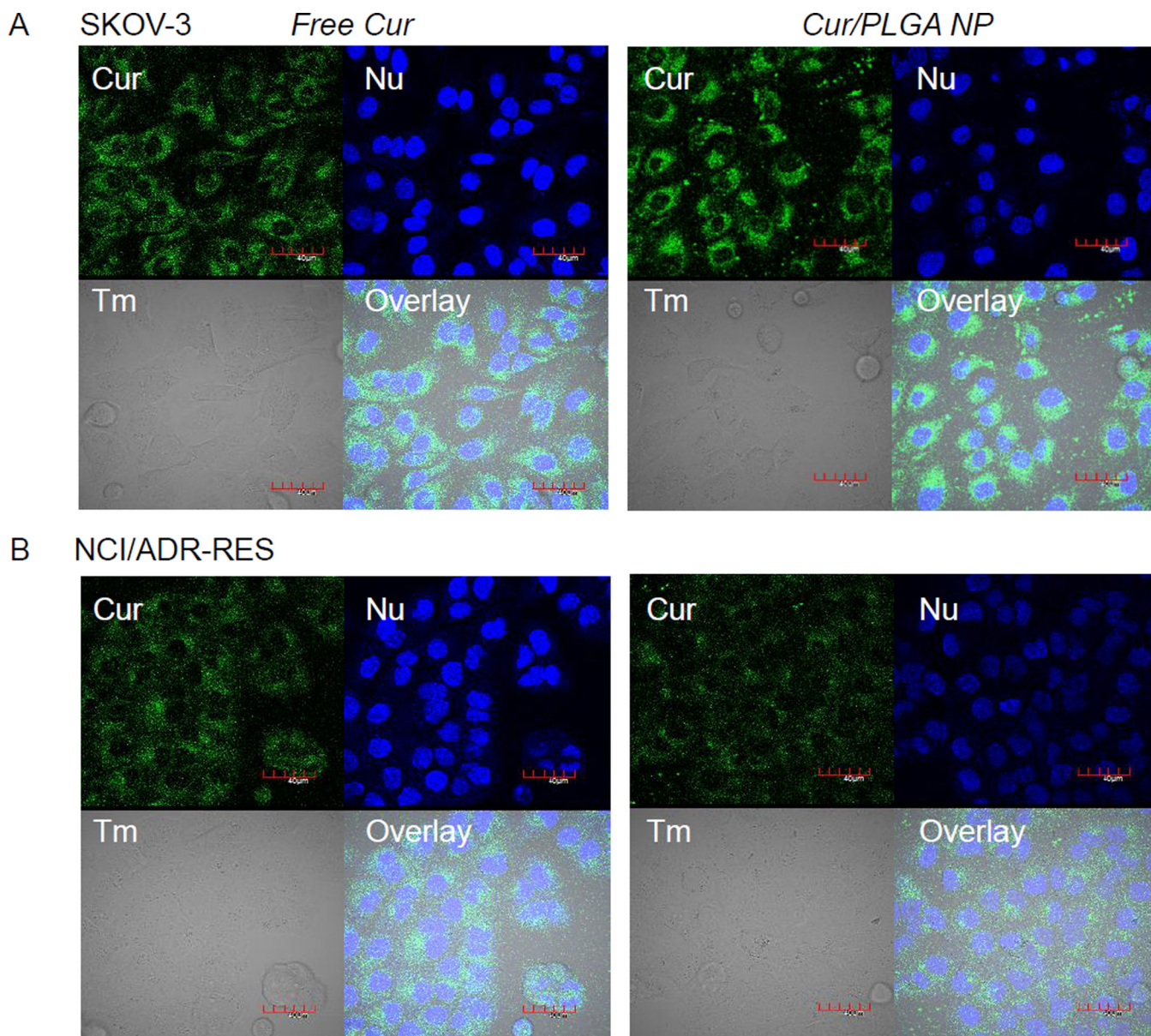


Fig. 4. (A) SKOV-3 cells and (B) NCI/ADR-RES cells incubated with free Cur or Cur/PLGA NPs for 3 hours. Free Cur entered both SKOV-3 and NCI/ADR-RES cells. Cells incubated with Cur/PLGA NPs also showed intracellular fluorescence signals. Cur: green fluorescence signal from Cur; Nu: nuclei stained with Draq5; Tm: transmission image; Overlay: overlay of NP, Nu and Tm. Magnification: 600 \times . Each scale bar = 40 μ m.

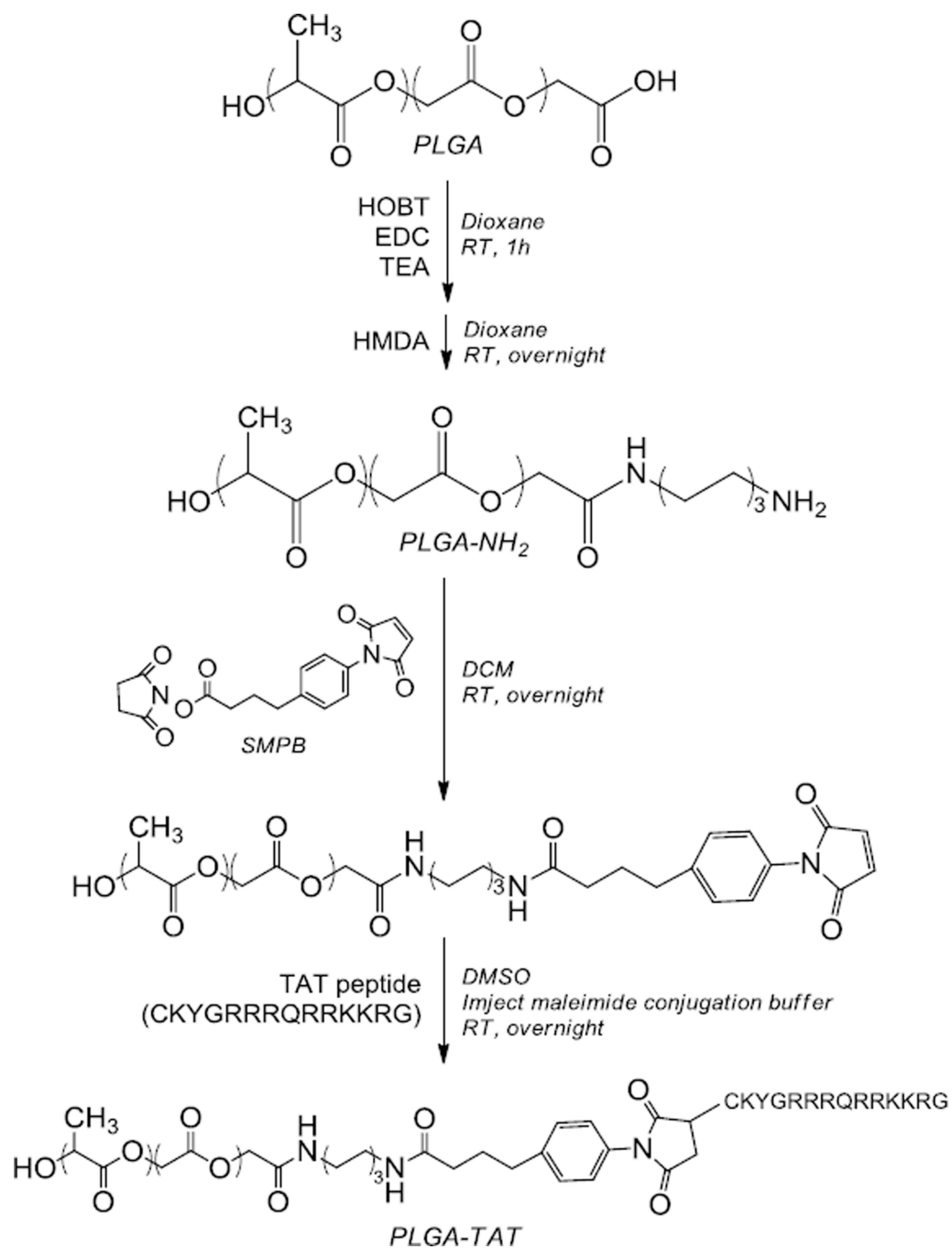


Table 1

Average sizes and zeta potentials of NPs.

Particle	Size (nm)	Surface charge (mV)
PLGA NPs	170 ± 6.1	-16 ± 3.5
PLGA-TAT NPs	225 ± 33	-9.8 ± 2.8
PTX/PLGA NPs	297 ± 55	-9.3 ± 4
PTX/PLGA-TAT NPs	250 ± 35	-15 ± 4.3

* Data represents an average ± standard deviation of at least 3 identically and independently prepared samples. PTX/PLGA NPs were significantly larger than PLGA NPs (ANOVA, Tukey test means comparison, $p < 0.05$). Other NPs were not significantly different from each other in size.